Journal of Material Science and Mechanical Engineering (JMSME)
p-ISSN: 2393-9095; e-ISSN: 2393-9109; Volume 10, Issue 2; April-June, 2023, pp. 112-117

http://www.krishisanskriti.org/Publication.html

Heave Motion Control of an Autonomous Underwater Vehicle Having Four Ballast Tanks

Srinjoy Das[1] and Pranibesh Mandal[2]

[1]UG Student, Department of Mechanical Engineering, Jadavpur University
[2]Assistant Professor, Department of Mechanical Engineering, Jadavpur University
E-mail: [1]srinjoydas78@gmail.com, [2]pranibesh.mandal@jadavpuruniversity.in

Abstract—*Autonomous Underwater Vehicles (AUVs) have a wide range of applications especially in underwater survey and defense operations along with industrial and military use. Heave motion has been a significant aspect of AUV dynamics and control of heave motion has been a topic of research for long. In most of the cases, a traditional submarine design is used to perform the motion analysis. Here, an underwater vehicle equipped with four ballast tanks at four bottom corners has been used and a closed loop model free controller has been developed to control the heave motion. PI and PID controller performances have been compared for different heave displacement signals with varying frequencies. The simulation results revealed excellent tracking throughout the cycle for sinusoidal and triangular displacements upto a frequency of 0.02 Hz.*

1. INTRODUCTION

Unmanned Underwater Vehicles (UUV) are submersible vehicles that can be used in underwater operations. They are particularly helpful in reducing risk to human life in deep underwater operations. UUVs are of two types: Remotely Operated Vehicles (ROV) and Autonomous Underwater Vehicles (AUV). ROV is a tethered underwater vehicle remotely operated by a human operator. AUV, on the other hand, is an untethered underwater vehicle that moves automatically without any direct input from an operator. AUVs are preferred over ROVs because of their energy efficiency. Kelasidi et al. compared the energy efficiency of underwater snake robots with that of ROVs with the help of a simulation study which showed that the former is more energy efficient for all the compared motion modes than the ROVs [1]. AUVs have immense use in ocean exploration, and industrial as well as military applications. Since they do not require any direct input from humans, AUVs can also be employed for underwater search and survey operations, underwater defense operations, an inspection of underwater objects, etc. [2]. One such application of AUV lies in the form of sea gliders which are operated remotely and are specifically designed for long-range missions [3].

Over the years, a lot of research and academic work has been conducted worldwide on the Motion Analysis and Control of AUVs using different control systems. Ferreira et al. deduced a dynamic model with six degrees of freedom of an underwater vehicle, considering all its physical characteristics of it [4]. Lin et al. built a prototype of a spherical underwater robot having three vectored water jet propellers as its propulsion system [5]. Inzartsev et al. proposed the motion control of an Autonomous Underwater Vehicle based on acoustic distance measuring systems [6]. Fan et al. worked on the motion analysis of AUV and cable coupling system to investigate the interaction between AUV and cable dynamic behaviors [7]. Healey et al. used a six DOF model for driving the underwater vehicle and also designed a multivariable sliding mode control for the combined steering, diving, and speed control functions [8]. Hai et al. built a petri-based recurrent type 2 fuzzy neural network to approximate the unknown and nonlinear dynamics of the AUV system [9]. Zhilenkov et al. built a fuzzy motion control system for an AUV [10]. Wan et al. improved the motion control and performance of AUV by using the fractional calculus ADRC strategy [11]. On the other hand, a saturation-based nonlinear fractional-order PD (FOPD) controller was proposed by Zhang et al. for motion control of AUV [12]. Kumar et al. proposed a subsurface mapping AUV with a modular-split hull design that provides better maneuverability than a conventional torpedo-shaped vehicle [13]. A new design for a high-maneuverability disc-shaped AUV was proposed by Wang et al. as a solution to the difficulty faced by vehicles in carrying out near-seabed operations due to poor maneuverability [14].

To improve the performance and robustness of AUVs, using a closed-loop control system of PID (Proportional, Integral, Derivative) type is more reliable than using an open-loop control system, especially in the presence of underwater disturbances. Experiments conducted by Alvarez et al. on Folaga showed that PID robust controllers improve effectiveness in the diving control phase [15]. Herlambang et al. proposed a Sliding PID Controller for AUV to analyze the surge and roll motion [16]. Gupta et al. built a miniature AUV having a non-conventional dual hull heavy bottom hydrodynamic design equipped with six thrusters and controlled it using a simple PID controller [17]. Park et al. used FGS and PD controllers to control the yaw and depth of an AUV [18]. A fractional-order PI controller helps in improving the system's performance and robustness [19]. This

FO PI control was extended further to fractional order PID by Wan et al. [20]. But all of the above works have proposed their motion analysis and control using a traditional submarine design. Moreover, a numeric study comparing the performance of PID to a proportional controller applied to the AUV linear model was proposed by Herlambang et al. [21]. However, such analysis between PID and PI controller is yet to be performed.

This paper proposes the motion analysis of an AUV equipped with four separate ballast tanks placed on four separate corners of the bottom side of the underwater vehicle and motion control of the same has been done using a Proportional-Integral-Derivative (PID) Controller. The motion analysis of the proposed underwater vehicle with ballast tanks, for heave motion, has been shown in the paper. A comparison has been made between the PI-Controller and PID-Controller performance of the system for linear, sinusoidal, and triangular demand inputs with variable frequencies. Consequently, the maximum operating frequencies for each of the demand types have been estimated for the optimum tracking performance of the controller.

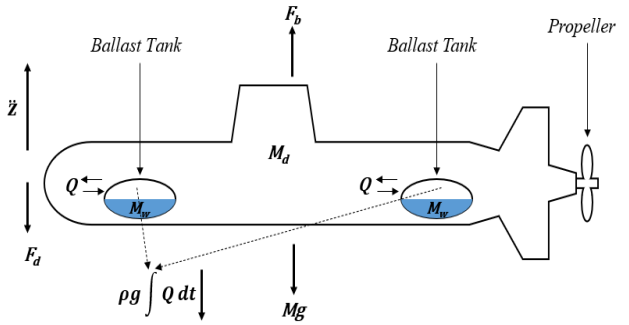

Fig. 1: Schematic of AUV for heave motion

2. SYSTEM DESCRIPTION & MODELLING

Fig. 1 demonstrates an Autonomous Underwater Vehicle (AUV) equipped with four separate ballast tanks placed on four separate corners of the bottom side of the underwater vehicle. The heave motion of the system has been governed by the entry and exit of water from the ballast tanks. The submarine has a dry mass M_d of 18.5 kg and a submerged volume SubVol of 0.02m^3. The propeller diameter D is 0.08 m. The values of density of water ρ, acceleration due to gravity g, discharge coefficient C_{dV}, vertical area of cross-section A_V, and horizontal area of cross-section A_H have been taken as$1029\ \text{kg/m}^3$,$9.81\ \text{m/s}^2$, 1, $0.1393\ \text{m}^2$ and $0.039732\ \text{m}^2$ respectively. Initially, the ballast tanks have been in half-filled condition and initially, the submarine has been at a depth $z_i$of 1m. The volume of a single ballast tank has been measured to be $0.001\ \text{m}^3$.

The submarine's dry mass M_d and initial mass of water in the ballast tanks M_w together taken as M, the volume flow rate of water entering and leaving the ballast tanks Q, buoyant force F_b, and drag force F_d have been used to determine the force balance equation for Heave Motion by balancing the forces acting on the system in the vertical direction. The forces acting along the vertical axis include the buoyant force F_b on the system acting upwards, the weight of the system Mg acting downwards, the weight of water entering and leaving the ballast tanks $\rho g \int Q\,dt$ in the downward direction, and drag force F_d acting in the direction opposite to that of motion, which yields

$$\left[M + \rho \int Q dt\right]\ddot{z} = F_b - Mg - \rho g \int Q\,dt - \frac{1}{2} C_{dV} \rho A_V \dot{z}|\dot{z}| \quad (1)$$

where,

$$M = M_d + M_w \quad (2)$$

$$F_b = \text{SubVol} * \rho * g \quad (3)$$

$$F_d = \frac{1}{2} C_{dV} \rho A_V \dot{z}|\dot{z}| \quad (4)$$

In (1), since Q denotes the volume flow rate of water entering as well as leaving the tanks, Q has been provided as a sinusoidal input. The positive region of the sinusoidal curve represents the case of water entering the ballast tanks and the negative region represents the case of water exiting the ballast tanks.

System Model for Heave Motion has been designed using the differential equation (1) in Matlab Simulink.Q is the input and displacement z, velocity $\dot{z}$, and acceleration $\ddot{z}$ of the system are obtained as outputs.

Motion control of the system has been first performed for a constant heave motion of the AUV. The block parameters of Q have been obtained by trial-and-error method from the Simulink Model such that the z vs t curve obtained for that Q is constant. The model has been run for a simulation time of 5000 s. Q has been given as a sine wave. The time period of the wave has been set to be T = 20 s, which is equivalent to a frequency of $2 * \text{pi} * 0.05\text{rad/s}$. The amplitude has been set at A = 0.001 m, phase = 0rad, and the bias has been obtained by trial-and-error method as b = 0.00001187 m.

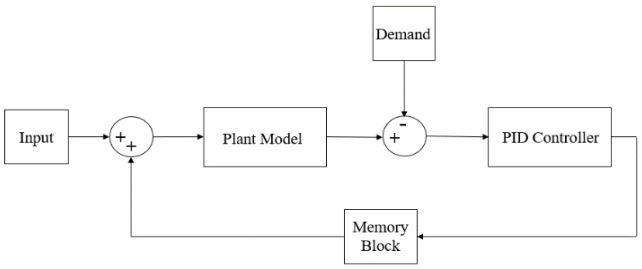

Fig. 2: Block diagram of PID control system

Since the z vs t curve obtained from the Simulink model is not constant throughout and has a net upward trend going forward, a Proportional-Integral-Derivative (PID) Controller has been

used for Heave Motion control of the underwater vehicle as demonstrated in Fig. 2. Motion analysis has been performed using P, PI, and PID-Controller. An ODE4 Runge Kutta solver of fixed step type with a step size of e-4 has been used. A comparison has been made for the motion analysis of the system between P and PI-Controller and between PI and PID-Controller for variable demand inputs with variable frequencies.

3. RESULTS AND DISCUSSION

The Heave Motion Simulink model serves as the transfer function for the P, PI, and PID-Controller. In P-Controller, there is only one gain value which is the Proportional Gain (K_p). The model has been tested for three ramp demands with slope values of 0, 0.001, and -0.001 respectively for a simulation time of 5000s. The purpose is to find K_p such that the response matches with the demand supplied and correspondingly the error tends to 0. The gain value for the P-Controller K_p has been taken as 0.005.

In PI-Controller, there are two gain values namely the Proportional Gain (K_p)and the Integral Gain (K_i). Ramp inputs with slopes equal to 0, 0.001, and -0.001 respectively with simulation time of 5000s have been provided as demands to determine the gain values. The gain values for the PI-Controller K_p and $K_i$have been taken as 0.9 and 0.008 respectively.

Figs. 3 and 4 demonstrate the displacement and % error comparison between P and PI-Controller for step demand, run for 10s and 100s respectively. The error in the case of the P controller fluctuates between -10% to +10% compared to -1.5% to +1.5% for PI and thus has been approximately seven times more compared to PI. In Figs. 5 to 8 which show a similar comparison but for positive ramp and negative ramp demands respectively, the fluctuations for P have been excessively higher than PI. Thus, due to such high error, the P-controller has been rejected and a motion analysis comparison has been carried out next using the PI and PID-Controller for obtaining more precise results.

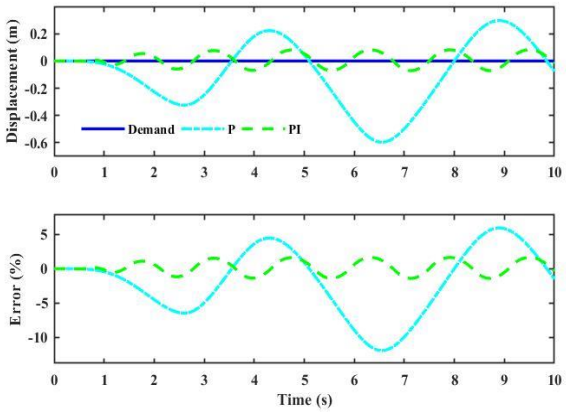

Fig. 3. Comparison of P and PI controller performances for step demand for a simulation time of 10s.

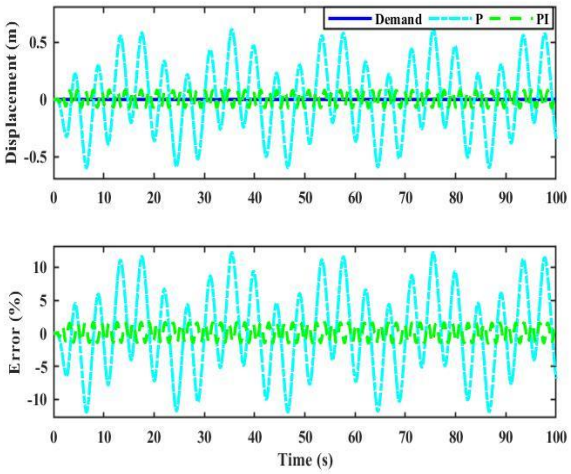

Fig. 4: Comparison of P and PI controller performances for step demand for a simulation time of 100s.

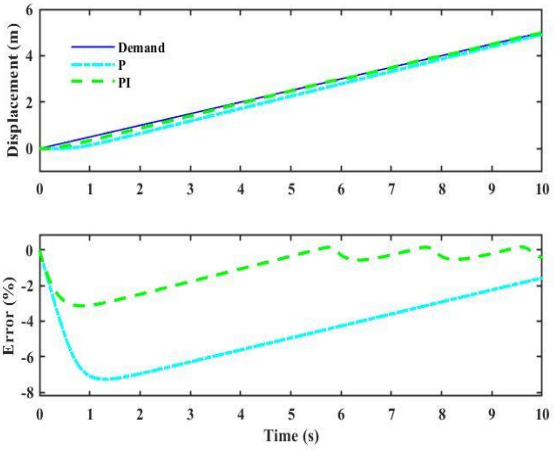

Fig. 5: Comparison of P and PI controller performances for positive ramp demand (slope=0.5) for a simulation time of 10s.

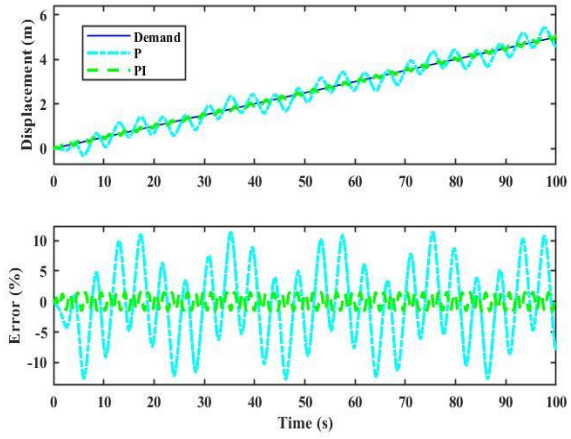

Fig. 6: Comparison of P and PI controller performances for positive ramp demand (slope=0.05) for a simulation time of 100s.

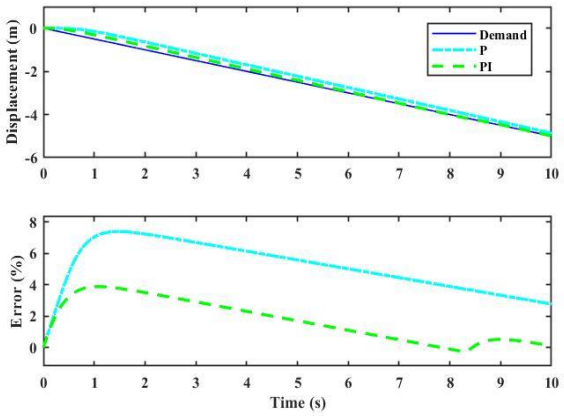

Fig. 7: Comparison of P and PI controller performances for negative ramp demand (slope=-0.5) for a simulation time of 10s.

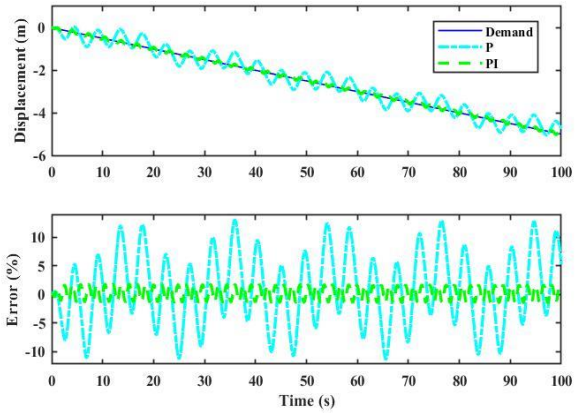

Fig. 8: Comparison of P and PI controller performances for negative ramp demand (slope=-0.05) for a simulation time of 100s.

In PID-Controller, along with the Proportional Gain (K_p)and Integral Gain (K_i), there is an additional gain value to be taken care of that is the Derivative Gain (K_d). The gain values for the PID-Controller K_p, K_i and K_d have been taken as 0.9, 0.008 and 0.2 respectively.

A comparative analysis has been performed between PI and PID-Controller for varied demand inputs. Figs. 9 and 10 demonstrate the displacement comparison between the demand and the corresponding response for PI and PID for a step demand for a simulation time of 10s and 100s respectively. The percentage error comparison shows that the error associated with PID control has been approximately ten times less than that for PI control. The error % for PID tends to be zero whereas, for PI, it fluctuates between -1.5 and 1.5%. In Figs. 11 and 12, displacement and error % comparison between PI and PID for positive ramp demand has been demonstrated for a displacement of 5m in 10s and 100s respectively. In Fig. 11, it can be seen that initially till around 5s, there has been a slight gap between the response and the demand line which decreases thereafter. The PI control in Fig. 11 has a significant error till 5.5s, after which it gradually decreases, and for PID, it extended till 4.5s after which the error gradually disappeared. A similar comparison has been provided in Figs. 13 and 14 for negative ramp demand.

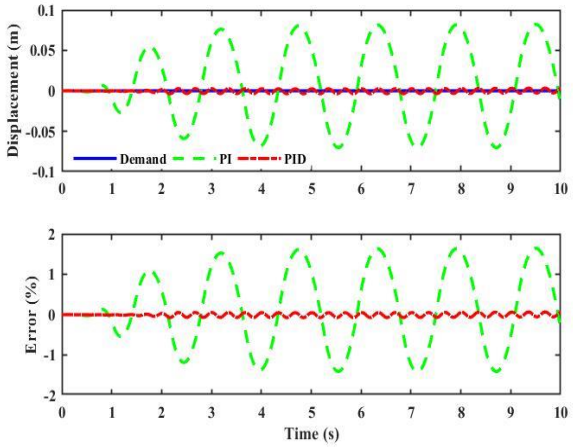

Fig. 9. Comparison of PI and PID controller performances for step demand for a simulation time of 10s.

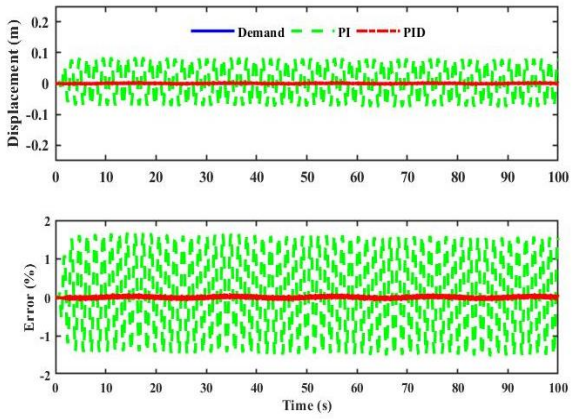

Fig. 10: Comparison of PI and PID controller performances for step demand for a simulation time of 100s.

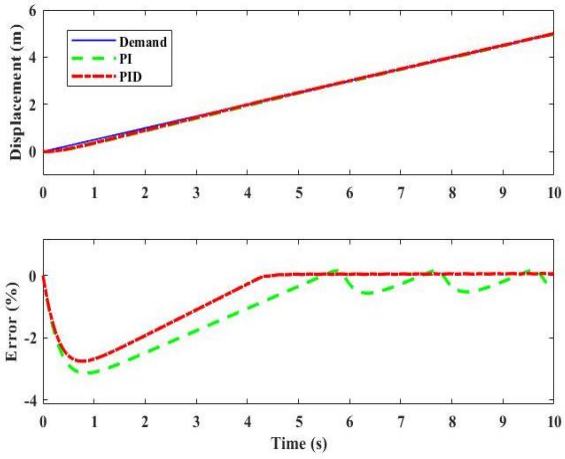

Fig. 11: Comparison of PI and PID controller performances for positive ramp demand (slope=0.5) for a simulation time of 10s.

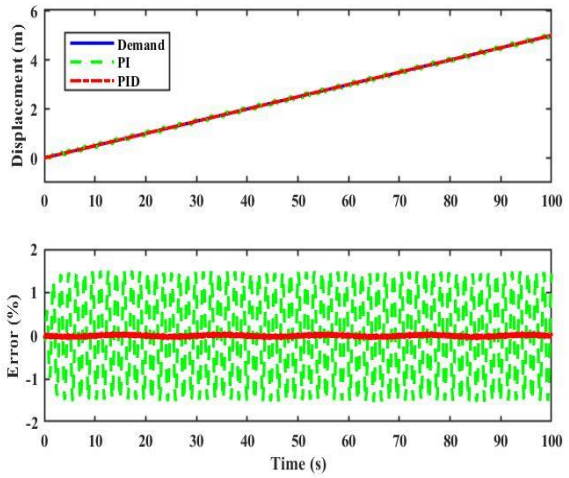

Fig. 12: Comparison of PI and PID controller performances for positive ramp demand (slope=0.05) for a simulation time of 100s.

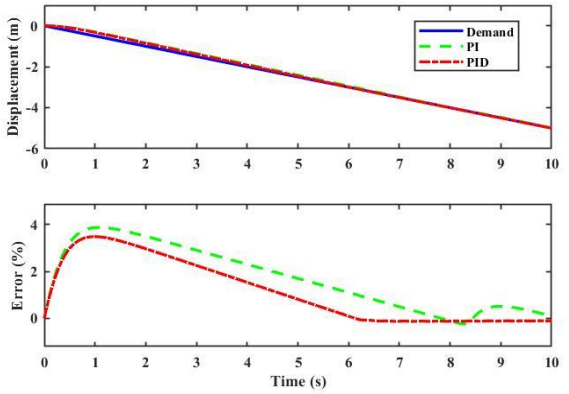

Fig. 13: Comparison of PI and PID controller performances for negative ramp demand (slope=-0.5) for a simulation time of 10s.

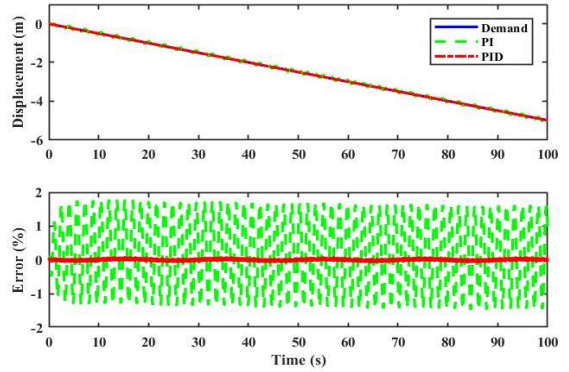

Fig. 14: Comparison of PI and PID controller performances for negative ramp demand (slope=-0.05) for a simulation time of 100s.

Fig. 15 demonstrates the comparison of displacement and error percentage between PI and PID for sinusoidal demand of frequencies 0.0004Hz, 0.002Hz, 0.004Hz, 0.01Hz, 0.02Hz and 0.04Hz respectively. The PID error percentage for Fig. 15 (a) to (d) have been almost constant and tend to be zero with the PI error oscillating between ±2 %, which results in the demand and response almost coinciding. On increasing the frequency to 0.02 Hz in Fig. 15 (e), both PI and PID error increases to ±10 %, which disturbs the almost perfect coincidence of the demand with the response. If the frequency has been increased further to 0.04 Hz in Fig. 15 (f), the error rises abruptly to ±100 %, due to which the controller has been unable to track the demand properly. As the frequency is increased, the tracking performance decreases and correspondingly the error percentage increases. Therefore, sinusoidal demands need to be operated at a frequency not more than 0.02 Hz, beyond which excess error occurs.

A similar comparative analysis for triangular demand with the same set of frequencies has been demonstrated in Fig. 16. Error level for frequency up to 0.004Hz in Fig. 16 (a) to (c) has been within ±2 % and increases to ±4 % for 0.01Hz in Fig.16 (d). The error fluctuates between ±7 % for 0.02Hz in Fig. 16 (e) and on increasing to 0.04Hz, fluctuation rises to approximately 10 times between ±70 % as demonstrated in Fig. 16 (f). Thus, the operating frequency for triangular demand has been within 0.02Hz, beyond which the tracking performance deteriorates significantly.

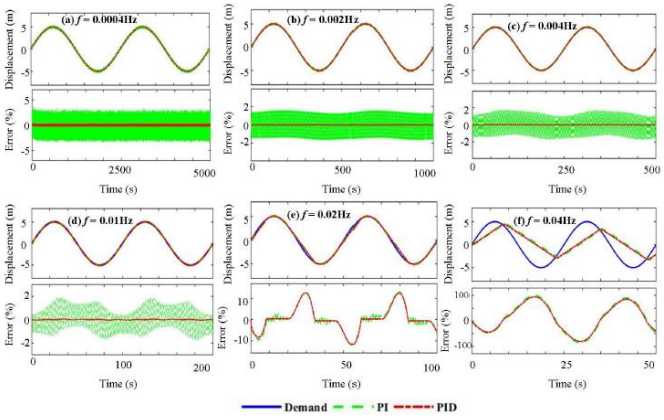

Fig. 15. Comparison of system response and error percentage between PI and PID controllers for sinusoidal demands of amplitude 5m and frequencies (a) 0.0004Hz (b) 0.002Hz (c) 0.004Hz (d) 0.01Hz (e) 0.02Hz (f) 0.04Hz

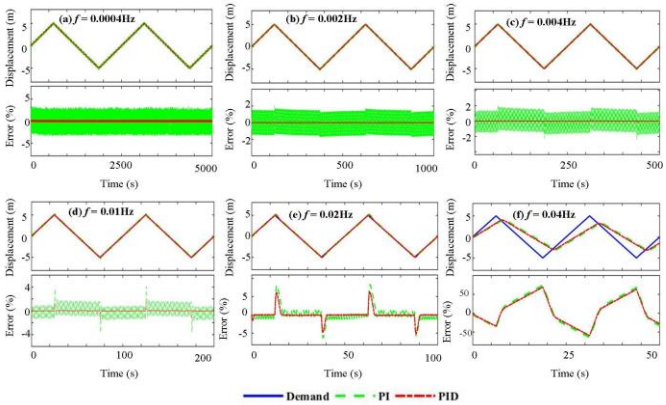

Fig. 16: Comparison of system response and error percentage between PI and PID controllers for triangular demands of amplitude 5m and frequencies (a) 0.0004Hz (b) 0.002Hz (c) 0.004Hz (d) 0.01Hz (e) 0.02Hz (f) 0.04Hz

4. CONCLUSION

Motion tracking control for heave displacement of an AUV have been studied in simulation frame. For different control demand types and frequencies, performances of P, PI and PID controllers have been compared. Both Pi and PID controllers have been found to have excellent tracking performance upto 0.02 Hz frequencies for both triangular and sinusoidal control demands. The step and ramp responses for these controller have also shown excellent tracking

REFERENCES

[1] Kelasidi, E., Pettersen, K. Y., & Gravdahl, J. T. (2015). Energy efficiency of underwater robots. IFAC-PapersOnLine, 48(16), 152-159.

[2] Alam, K., Ray, T., &Anavatti, S. G. (2014). Design and construction of an autonomous underwater vehicle. Neurocomputing, 142, 16-29.

[3] Eriksen, C. C., Osse, T. J., Light, R. D., Wen, T., Lehman, T. W., Sabin, P. L., ... & Chiodi, A. M. (2001). Seaglider: A long-range autonomous underwater vehicle for oceanographic research. IEEE Journal of oceanic Engineering, 26(4), 424-436.

[4] Ferreira, B., Pinto, M., Matos, A., & Cruz, N. (2009, October). Control of the MARES autonomous underwater vehicle. In OCEANS 2009 (pp. 1-10). IEEE.

[5] Lin, X., Guo, S., Tanaka, K., & Hata, S. (2011, May). Development of a spherical underwater robot. In The 2011 IEEE/ICME International Conference on Complex Medical Engineering (pp. 662-665). IEEE.

[6] Inzartsev, A., Kiselyov, L., Medvedev, A., Pavin, A., & Casolo, F. (2010). Autonomous Underwater Vehicle Motion Control during Investigation of Bottom Objects and Hard-to-Reach Areas. In Motion Control (pp. 590-228). In-Tech Publishers.

[7] Fan, S., Chan, K., & Chin, C. K. (2020). Motion analysis of an autonomous underwater vehicle tethered with an optical fiber for real-time surveillance. IEEE Journal of Oceanic Engineering, 46(2), 434-446.

[8] Healey, A. J., & Lienard, D. (1993). Multivariable sliding mode control for autonomous diving and steering of unmanned underwater vehicles. IEEE journal of Oceanic Engineering, 18(3), 327-339.

[9] Hai, H., Guocheng, Z., Hongde, Q., &Zexing, Z. (2017). Autonomous underwater vehicle precise motion control for target following with model uncertainty. International Journal of Advanced Robotic Systems, 14(4), 1729881417719808.

[10] Zhilenkov, A., Chernyi, S., & Firsov, A. (2021). Autonomous underwater robot fuzzy motion control system with parametric uncertainties. Designs, 5(1), 24.

[11] Wan, J., Liu, H., Yuan, J., Shen, Y., Zhang, H., Wang, H., & Zheng, Y. (2021). Motion Control of Autonomous Underwater Vehicle Based on Fractional Calculus Active Disturbance Rejection. Journal of Marine Science and Engineering, 9(11), 1306.

[12] Zhang, L., Liu, L., Zhang, S., & Cao, S. (2019). Saturation based nonlinear FOPD motion control algorithm design for autonomous underwater vehicle. Applied Sciences, 9(22), 4958.

[13] Kumar, V. S., & Rajagopal, P. (2021). Modelling and Analysis of Turning Motion of a Subsurface Mapping AUV with Split-Hull Design. Journal of Marine Science and Application, 20(2), 284-301.

[14] Wang, Z., Liu, X., Huang, H., & Chen, Y. (2019). Development of an autonomous underwater helicopter with high maneuverability. Applied Sciences, 9(19), 4072.

[15] Alvarez, A., Caffaz, A., Caiti, A., Casalino, G., Gualdesi, L., Turetta, A., & Viviani, R. (2009). Folaga: A low-cost autonomous underwater vehicle combining glider and AUV capabilities. Ocean engineering, 36(1), 24-38.

[16] Herlambang, T., &Nurhadi, H. (2017). Design of a sliding pid controller for the surge and roll motion control of unusaitsauv. IJCSAM (International Journal of Computing Science and Applied Mathematics), 3(2), 61-64.

[17] Upadhyay, V., Gupta, S., Dubey, A. C., Rao, M. J., Siddhartha, P., Gupta, V., ... &Idichandy, V. G. (2015, February). Design and motion control of autonomous underwater vehicle, Amogh. In 2015 IEEE Underwater Technology (UT) (pp. 1-9). IEEE.

[18] Park, R. E., Hwang, E. J., Lee, H. J., & Park, M. (2010). Motion control of an AUV (Autonomous Underwater Vehicle) using fuzzy gain scheduling. Journal of Institute of Control, Robotics and Systems, 16(6), 592-600.

[19] Liu, L., Zhang, L., & Zhang, S. (2021). Robust PI λ controller design for AUV motion control with guaranteed frequency and time domain behaviour. IET Control Theory & Applications, 15(5), 784-792.

[20] Wan, J., He, B., Wang, D., Yan, T., & Shen, Y. (2019). Fractional-order PID motion control for AUV using cloud-model-based quantum genetic algorithm. IEEE Access, 7, 124828-124843.

[21] Herlambang, T., &Nurhadi, H. (2018). Design of motion control using proportional integral derivative for unusaitsauv. International Review of Mechanical Engineering (I. RE. ME), 12(11), 928-938.